Shape Analysis of the Left Ventricular Endocardial Surface and Its Application in Detecting Coronary Artery Disease

Anirban Mukhopadhyay[1], Zhen Qian[2], Suchendra Bhandarkar[1], Tianming Liu[1], and Szilard Voros[2]

[1] Department of Computer Science, The University of Georgia, Athens, GA 30602-7404, USA
[2] Piedmont Heart Institute, Atlanta, GA 30309, USA

Abstract. Coronary artery disease is the leading cause of morbidity and mortality worldwide. The complex morphological structure of the ventricular endocardial surface has not yet been studied properly due to the limitations of conventional imaging techniques. With the recent developments in Multi-Detector Computed Tomography (MDCT) scanner technology, we propose to study, in this paper, the complex endocardial surface morphology of the left ventricle via analysis of Computed Tomography (CT) image data obtained from a 320 Multi-Detector CT scanner. The CT image data is analyzed using a 3D shape analysis approach and the clinical significance of the analysis in detecting coronary artery disease is investigated. Global and local 3D shape descriptors are adapted for the purpose of shape analysis of the left ventricular endocardial surface. In order to study the association between the incidence of coronary artery disease and the alteration of the endocardial surface structure, we present the results of our shape analysis approach on 5 normal data sets, and 6 abnormal data sets with obstructive coronary artery disease. Based on the morphological characteristics of the endocardial surface as quantified by the shape descriptors, we implement a Linear Discrimination Analysis (LDA)-based classification algorithm to test the effectiveness of our shape analysis approach. Experiments performed on a strict leave-one-out basis are shown to achieve a classification accuracy of 81.8%.

Keywords: Ventricular endocardial surface, cardiovascular CT, shape analysis.

1 Introduction

Coronary artery disease or *atherosclerosis* is the most common cause of morbidity and mortality worldwide. Atherosclerosis eventually leads to formation of plaques that cause arterial stenosis and chronic myocardial ischemia and in some cases, acute myocardial infraction. Anatomic and imaging studies have revealed that, instead of a simple and smooth surface, the endocardial surface of the heart ventricle is composed of a complex structure of *trabeculae carneae*, which are small muscular columns that arise naturally from the inner surface of the ventricles. Alterations in the ventricular trabeculation have been found to closely associate with some cardiovascular diseases,

D.N. Metaxas and L. Axel (Eds.): FIMH 2011, LNCS 6666, pp. 275–283, 2011.

such as myocardial noncompaction disease [1] and hypertrophy [2]. However, due to the limitations in the spatial resolution of conventional *in-vivo* imaging techniques, very few research studies have been undertaken to study the ventricular trabeculation at a detailed level, and investigate the relationship between structural changes in ventricular trabeculation and certain cardiac pathologies.

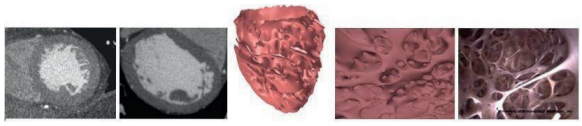

(a) (b) (c) (d) (e)

Fig. 1. Illustration of endocardial surface reconstruction using high-resolution CT data, and the comparison with an *ex vivo* picture of a live beating heart. (a, b) are two sample images of the CT data used in this study. (c) depicts the endocardial surface segmentation results for a whole left ventricle. (d) is an enlarged area near the reconstructed ventricular apex. Notice its surprising similarity with the apical structure in the *ex vivo* picture of a live beating heart (e) [10].

Owing to the recent developments in cardiovascular imaging using Multi-Detector Computed Tomography (MDCT) scanners, it is possible for contrast-enhanced Computed Tomography (CT) images to achieve an isotropic image resolution of less than 0.5mm. As shown in Fig. 1, it is possible to observe the detailed structure of the ventricular trabeculation using such high-resolution CT images. In [3], a deformable model-based segmentation method was developed to reconstruct a very detailed anatomy of the left ventricle. In [4], by using high-resolution CT, papillary muscles were found to be attached to the *trabeculae carneae*, but not directly to the myocardium. These studies suggest that a closer look at the detailed trabecular structure may lead to new understandings of the cardiac anatomy, function and pathology.

With the introduction of the new 320-MDCT scanner, we are able to scan the heart in a single heart beat, so as to eliminate the artifacts introduced by misalignment between cardiac segments that are acquired during different heart beats on conventional 64- or 256-MDCT scanners. The endocardial surface structure recovered from the image data acquired with a 320-MDCT scanner would be potentially more accurate and reliable.

In this paper, we have developed an image segmentation and shape analysis framework to study the endocardial surface of the left ventricle from contrast-enhanced CT images acquired using a 320-MDCT scanner. In order to handle the complex topological changes of the endocardial surface, we employed a 3D level set-based approach for segmentation of the endocardial surface. Since the trabecular structure varies in different locations of the ventricle, we further divided the endocardial surface of the left ventricle into 17 segments according to the standard American Heart Association (AHA) model [5] for more localized shape analysis.

In each of the 17 ventricular segments, we adapted two different descriptors for analysis of the shape of the endocardial surface: a D2 descriptor [6] and a shape index described in [7] [8]. These two shape descriptors describe the shape patterns of the myocardial surface in terms of either global or local details. In order to show the

effectiveness of the shape analysis based on the above shape descriptors, we collected 11 MDCT data sets obtained from 6 abnormal hearts of subjects with obstructive coronary heart disease, and 5 normal hearts from healthy subjects. We employed our segmentation and shape analysis procedures on each data set to compute a characteristic shape matrix for the left ventricle. A Linear Discriminant Analysis (LDA)-based classifier [11] was implemented to classify the abnormal hearts from the normal ones using the characteristic shape matrices on a strict leave-one-out basis. Experimental results showed that 9 out 11 data sets were classified correctly, which is a very promising result.

The remainder of the paper is organized as follows. In Section 2, we describe our segmentation and shape analysis methods in detail. In Section 3, we present experimental results on the previously described MDCT data sets. In Section 4, we conclude the paper with a brief discussion about our approach and propose some directions for future work.

2 MDCT Image Segmentation and Ventricular Shape Analysis

2.1 Left Ventricle Segmentation and Meshing

There are three types of *trabeculae carneae* morphologies: some are attached along their entire length to the ventricular wall and form prominent ridges; some are fixed at their extremities but free in the middle; and others connect the root of the papillary muscles and the ventricular wall. Consequently, the endocardial surface of the left ventricle does not possess a simple topology. In order to adapt to the topological changes caused by the complex structure of the trabeculation, we adapted a 3D level set-based approach to segment the endocardial surface of the left ventricle. In order to suppress noise and still retain the shape-defining edges in the CT image data, we employed a median filter-based denoising procedure on the 3D CT data prior to segmentation. The size of the median filter was empirically set to 7×7 based on our CT data set. The level set-based segmentation procedure without reinitialization as proposed by Li et al. [9] was applied to the median-filtered 3D image data set. The subsequent denoising via the mean face normal filtering procedure proposed by Zhang et al. [12] was used to obtain the smooth shape of the myocardial surface of the left ventricle.

2.2 Shape Description

The next step after segmentation and meshing of the raw input CT image data is to characterize the shape of the left ventricle. We have considered two primary shape descriptors in this paper. One is relatively straight forward, i.e., the D2 shape descriptor proposed by Osada et al. [6]. The other is the 3D shape index first introduced by Koenderink [7] and later modified by Zaharia and Preteux [8].

The D2 shape descriptor is a global shape descriptor. It is the shape signature of a 3D object represented as a probability distribution. The probability distribution is obtained via sampling of a pre specified shape function that measures a geometric property of the 3D shape. The shape function for D2 is the distance between two random points on the 3D surface of the object. In the context of our problem, two

large random samples of vertices are generated from the mesh-based representation and the distance between each pair of vertices (where each vertex in the pair belongs to a different sample) is calculated. The underlying idea is to transform the shape into a parameterized probability distribution function where the probability distribution is deemed to represent the global shape.

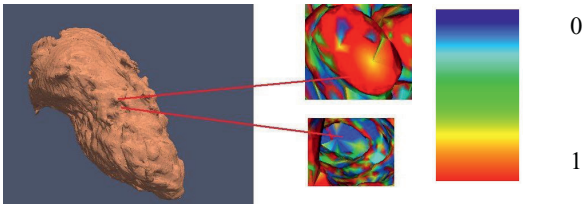

Fig. 2. Illustration of the accuracy of shape index. The peak is shown in red with shape index value close to 1 whereas the pit of just beside the peak has value close to 0 and shown in blue.

The second shape descriptor, i.e., the *shape index*, describes the local shape of the mesh based on the surface curvature computed in a local neighborhood of the surface point (Fig. 2). The shape index of a surface point is defined as a function of the two local principal surface curvatures. Let p be a point on a 3D surface and let the principal curvatures associated with point p be denoted by k_p^1 and k_p^2 where, $k_p^1 > k_p^2$. The shape index at point p, denoted by I_p, is defined as:

$$I_p = \frac{1}{2} - \frac{1}{\Pi}\arctan\left(\frac{k_p^1 + k_p^2}{k_p^1 - k_p^2}\right)$$

The shape index is a local geometric attribute of the 3D surface. The values of the shape index lie in the interval [0, 1]. The shape index value is not defined for planar surfaces. The shape index provides a scale for representing basic elementary shapes such as *convex, concave, rut, ridge* and *saddle* [8]. The shape index value is invariant to scale and 3D rigid-body transformation (i.e., translation and rotation) in Euclidean space.

The shape of the myocardial surface is observed to exhibit both, global structure as well as detailed local structure. Since there have been no previous studies detailing which of the shape properties (local or global) convey more valuable clinical information, we considered both local and global shape descriptors for this study.

2.3 Data Preparation

In order to ensure a better comparison between different analysis methods, the AHA has been published recommendations for standardized myocardial segmentation [5]. In this paper, we adapted an AHA 17-segment model [5] to divide the left ventricle into 17 segments for better localized shape analysis. The long axis of the left ventricle was determined followed by the division of the left ventricle into 4 main segments,

i.e., *apex, apical, mid cavity* and *basal* along the longitudinal orientation. Division of the endocardial surface in the short axis view was tackled by exploiting knowledge of the cardiac anatomy. Three landmark points were considered across the septum based on which the apical was subdivided into four segments and the mid cavity and basal into six segments. Finally, each left ventricular endocardial surface was divided into 17 segments per the standard AHA model [5].

3 Experimental Results

The proposed methods for segmentation, meshing and shape description were employed on 11 MDCT data sets consisting of 6 data sets from cardiac patients and 5 from normal subjects. In the case of the cardiac patients, incidence of single-vessel or multi-vessel obstructive disease was found in the four major coronary arteries using X-ray angiography, which was further confirmed by myocardial perfusion and fractional flow reserve tests.

Each of the cardiac patients and normal subjects was subject to a contrast-enhanced CT scan on a 320-MDCT scanner using a standard CT angiography protocol with ECG gating. The resulting images were reconstructed at 75% in the R-R cycle to ensure that all data were acquired during the same cardiac phase with minimal ventricular motion. This ensures that the subsequent shape analysis is minimally affected by the cardiac motion. All topologically correct and geometrically accurate data are generated via the segmentation method described in Section 2.1. The atria and valves were removed from the segmented ventricular meshes.

3.1 Segmentation Results

The result of the segmentation of the left ventricle is shown in Fig. 3. It can be easily seen that the segmented result is reasonably good with the spatial details of the myocardial surface left intact although the noise in the data is substantially filtered. Fig. 4 shows the division of the left ventricle into the septal and free wall halves. We observe that the spatial distribution of the trabeculation varies with location within the ventricle; the free wall tends to have more trabeculation whereas the septum tends to

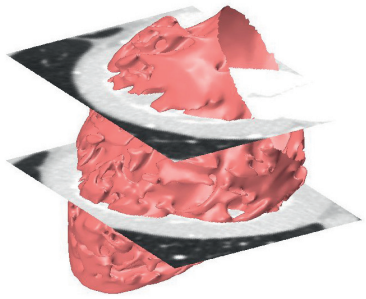

Fig. 3. Illustration of the segmentation result and accuracy of the method described in Section 2.1

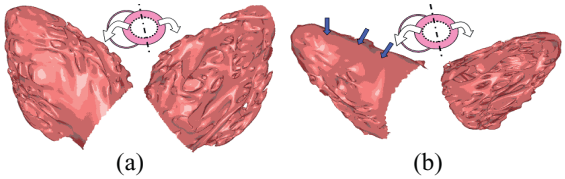

Fig. 4. The left ventricular endocardial surface segmentation meshes were dissected into two halves, the septum (on the left) and the free wall (on the right). (a) is from a normal heart, and (b) is from a diseased heart. In a normal heart, the trabeculation is seen to vary with location; the septum is smoother than the free wall. In the diseased heart, notice the loss of trabeculation in the septal area indicated by the blue arrows. This loss of trabeculation may be associated with obstructive disease in the left anterior descending artery, which supplies blood to the anteroseptal heart wall.

be smoother, which is the precise rationale for using the AHA 17-segment model to perform a localized shape analysis. Furthermore, by using the proposed segmentation approach, it is possible to even visually distinguish the difference in trabeculation between normal and diseased hearts. These results are sufficient to prove that the proposed segmentation method is fairly standard and may work well for subsequent quantitative shape analysis.

3.2 Shape Description Results

The shape description results are shown as histograms in Fig. 5 for the D2 shape descriptor and shape index. Each histogram has 20 bins in the horizontal direction in the range [0, 1] and corresponding number of vertices in the vertical direction. The normal hearts are represented in red and the diseased hearts in blue for both the diagrams. Fig. 5 clearly shows that information derived from the D2 shape descriptor is inadequate for distinguishing between normal and diseased hearts. This is because

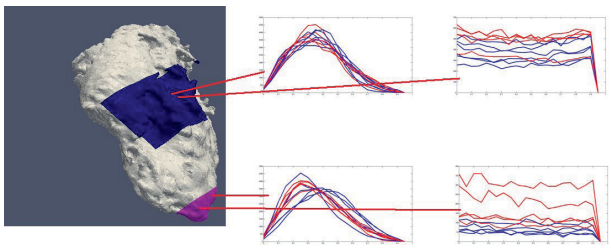

Fig. 5. Illustration to compare the results generated by D2 (b) and the shape index (c) for the ventricular segment 11 (blue) and ventricular segment 17 (pink) of the left ventricle (a). The normal left ventricles are represented in red and the diseased ones are represented in blue in the histogram.

the D2 shape descriptor is a global shape descriptor that does not capture the local spatial details of the underlying shape. On the other hand, the shape index is a local shape descriptor which successfully captures the local shape details. In Fig. 6, the difference in shape between the normal and diseased hearts is clearly visible in 17×20 dimensions (17 segments per left ventricle×1 histogram per segment×20 bins per histogram) which in turn confirms that for the type of application considered in this paper, local shape descriptors convey much more information than global ones.

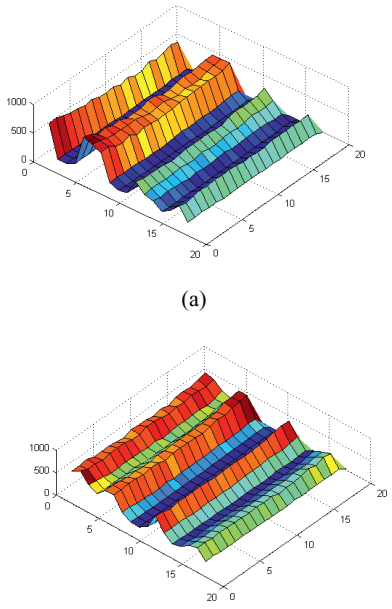

(a)

(b)

Fig. 6. Illustration to compare the results generated by the shape index for a diseased (a) vs. normal (b) left ventricular endocardial surface in 17×20 dimensions. The difference is clearly visible.

3.3 Classification Accuracy

In the appearance-based recognition paradigm, Linear Discriminant Analysis (LDA) [11] is a natural choice for classification. A typical two-class classifier can learn to separate the normal training samples from the abnormal samples by finding a proper projection function. LDA is a popular classification method that maximizes the between-class scatter defined by $\sum_{j=1}^{c}(\ _j - \ )(\ _j - \ )^T$ and minimizes the within-class scatter defined by $\sum_{j=1}^{c}\sum_{i=1}^{N_j}(x_i^j - \ _j)(x_i^j - \ _j)^T$ where is the mean of all classes, x_i^j is the ith sample of the jth class, $\ _j$ is the mean of jth class, N_j is the number of

samples in the jth class and c is the number of classes. LDA projects the $17 \times 20 = 340$-dimensional feature vector to a subspace of c-1 dimensions. Since in this application, c = 2 (i.e., normal and diseased), the 340-dimensional vector was projected onto a 1D scalar. Classification was done using a k-nearest neighbor (k-NN) scheme in the 1D subspace. We empirically tested the classifier for k = 1 and 3, and obtained the same result: 9 out of 11 samples were classified correctly. Table 1 shows the confusion matrix where 5 out of 6 diseased hearts and 4 of the 5 normal hearts were diagnosed correctly.

Table 1. Confusion matrix to illustrate the prediction accuracy

	Predicted Diseased	Predicted Normal
Actual Diseased	5	1
Actual Normal	1	4

4 Disccussion and Conclusions

To the best of our knowledge, this paper is amongst the earliest works that studies the endocardial surface structure of the left ventricle using a shape analysis approach with high-resolution CT input data, and demonstrates its potential predictive/diagnostic value for coronary artery disease. We can speculate that the success of our approach may lead to some functional implications. The presence of obstructive coronary arterial disease and perfusion defects in patients reveals ischemia in the corresponding regions of the myocardium. The ischemic myocardium loses contractibility and has a tendency to get stiffer and be pushed outward by the high ventricular blood pressure. Such changes in the underlying myocardium may be the reason for changes in the trabeculation pattern and endocardial surface morphology that we have discovered in our analysis. This association between the cardiac shape features (i.e., cardiac morphology) and cardiac functionality will be explored in our future work.

References

[1] Goo, S., Joshi, P., Sand, G., Gerneke, D., Taberner, A., Dollie, Q., LeGrice, I., Loiselle, D.: Trabeculae Carneae as Models of the Ventricular Walls: Implications for the Delivery of Oxygen. Jour. Gen. Physiology 134(4), 339–350 (2009)

[2] Agmon, Y., Connoll, H.M., Olson, L.J., Khandheria, B.K., Seward, J.B.: Noncompaction of the Ventricular Myocardium. Jour. Amer. Soc. Echocardiography 12(10), 859–863 (1999)

[3] Chen, T., Metaxas, D.N., Axel, L.: 3D Cardiac Anatomy Reconstruction Using High Resolution CT Data. In: Barillot, C., Haynor, D.R., Hellier, P. (eds.) MICCAI 2004. LNCS, vol. 3216, pp. 411–418. Springer, Heidelberg (2004)

[4] Axel, L.: Papillary Muscles Do Not Attach Directly to the Solid Heart Wall. Circulation 109, 3145–3148 (2004)

[5] Cerqueira, M.D., Weissman, N.J., Dilsizian, V., Jacobs, A.K., Kaul, S., Laskey, W.K., et al.: Standardized Myocardial Segmentation and Nomenclature for Tomographic Imaging of the Heart. Circulation 105, 539–542 (2002)

[6] Osada, R., Funkhouser, T., Chazelle, B., Dobkin, D.: Shape Distributions. ACM Trans. Graphics 21(4), 807–832 (2002)
[7] Koenderink, J.: Solid Shape. The MIT Press, Cambridge (1990)
[8] Zaharia, T., Preteux, F.: 3D Shape-based Retrieval Within the MPEG-7 Framework. In: Proc. SPIE Conf. Nonlinear Image Processing and Pattern Analysis XII, vol. 4304, pp. 133–145 (2001)
[9] Li, C., Xu, C., Gui, C., Fox, M.D.: Level Set Evolution Without Re-initialization: A New Variational Formulation. In: Proc. IEEE Conf. CVPR 2005, vol. 1, pp. 430–436 (2005)
[10] Medtronic Inc. The Visible Heart webpage, http://www.visibleheart.com/index.shtml
[11] Martinez, A.M., Kak, A.C.: PCA versus LDA. IEEE Trans. Pattern Analysis and Machine Intelligence 23(2), 228–233 (2001)
[12] Zhang, Y., Hamza, A.B.: Vertex-based Diffusion for 3-D Mesh Denoising. IEEE Trans. Image Processing 16(4), 1036–1045 (2007)